Review

For reprint orders, please contact: reprints@futuremedicine.com

Regenerative Medicine

Advances in on-chip vascularization

Microfluidics is invaluable for studying microvasculature, development of organ-on-chip models and engineering microtissues. Microfluidic design can cleverly control geometry, biochemical gradients and mechanical stimuli, such as shear and interstitial flow, to more closely mimic *in vivo* conditions. *In vitro* vascular networks are generated by two distinct approaches: via endothelial-lined patterned channels, or by self-assembled networks. Each system has its own benefits and is amenable to the study of angiogenesis, vasculogenesis and cancer metastasis. Various techniques are employed in order to generate rapid perfusion of these networks within a variety of tissue and organ-mimicking models, some of which have shown recent success following implantation *in vivo*. Combined with tuneable hydrogels, microfluidics holds great promise for drug screening as well as in the development of prevascularized tissues for regenerative medicine.

Kristina Haase[1] & Roger D Kamm*[,1,2,3]

[1]Department of Mechanical Engineering, MIT, Cambridge, MA, USA
[2]Department of Biological Engineering, MIT, Cambridge, MA, USA
[3]Singapore MIT Alliance for Research & Technology, Singapore, Singapore
*Author for correspondence: rdkamm@mit.edu

First draft submitted: 14 October 2016; Accepted for publication: 24 January 2017; Published online: 20 March 2017

Keywords: angiogenesis • microfluidics • microvasculature • organ-on-a-chip • permeability • regenerative medicine • tissue-engineering • vasculogenesis

Microvasculature function is of key importance in the fields of tissue engineering and regenerative medicine. Despite success with *in vivo* implantation of thin and/or avascular engineered tissues such as skin and cartilage, generating highly vascularized thick tissues *in vitro* remains a significant challenge [1]. Thick engineered tissues require functional microvascular networks to provide adequate gas and nutrient exchange, as well as waste removal. The last few decades have brought about significant advances in our understanding of human vascular growth during development and adulthood, as well as its implications in pathologies, particularly cancer. Microfluidic models have contributed significantly to our understanding of how microvascular networks form and respond to a myriad of biochemical and mechanical signals. Combining microfluidic approaches and prevascularization methods is one promising strategy toward engineering of functional tissues. Following a brief summary of *in vivo* blood vessel formation, this review highlights exemplary microfluidics-based models employing patterned and self-assembly methods toward the study of angiogenesis and vasculogenesis. We address such questions as: What defines a functional *in vitro* network? What microenvironment and mechanical controls are necessary to realistically mimic native networks? We then offer our perspective on how microfluidic models can bridge the gap between micro- and macro-scales by discussing organ-on-chip models. Finally, we discuss how the use of microfluidic techniques, along with novel hydrogels, will promote the development of vascularized engineered tissues.

Blood vessel formation *in vivo*

The formation and maintenance of our vascular system is of crucial importance both during development and throughout our adult lives. Blood vessel formation during early embryogenesis relies on angiogenic cell

Future Medicine part of fsg

coalescence, followed by formation of hollow cannules. Early capillary-like networks form from angioblasts that differentiate into endothelial cells (ECs), a process known as vasculogenesis (Figure 1A). Vasculogenesis also occurs during adulthood through recruitment of ECs from bone marrow. During development, and following the formation of a primary network, expansion and sprouting occurs from existing vessels by a process known as angiogenesis (Figure 1B & D). Vessels form by growth, proliferation, alignment, tube formation and, finally, they anastomose with surrounding vessels. Endothelium is a key component of vessels of both macro- and micro-scales. An endothelial monolayer creates a dynamic barrier that, in larger vessels, is surrounded by smooth muscle cells (SMCs) and an extracellular matrix (ECM) mostly comprised collagen and elastin. The endothelium acts as a selectively permeable barrier between circulating blood and surrounding tissues, is a thrombogenic barrier, and regulates vasodilation and vessel formation (Figure 1C–E). Both pericytes (microvasculature) and SMCs (larger vessels) play a role in stabilization and growth control. A detailed description of these processes can be found in the review by Herbert and Stainier [2].

Angiogenic sprouting is vital for delivery of nutrients and gas exchange to ischemic regions and is essential in tissue remodeling, regeneration and in solid tumor growth [4]. During angiogenesis, ECs degrade the ECM by MMPs, enabling the growth of new vessel sprouts, regulated by a variety of signaling molecules, adhesion proteins, growth factors and inhibitors (pro- and anti-angiogenic factors are listed in [5]; Figure 1D). Above all, VEGF is rate-limiting in physiological angiogenesis (reviewed in [3]). The most abundant form of VEGF-A, $VEGF_{165}$, is released by fibroblasts, monocytes, macrophages and lymphocytes to act as a mitogen of ECs. Activated oncogenes, cytokines and hypoxia, are known stimulants of VEGF expression [6]. The release of HIF-1 initiates transcription of VEGF (among others) in hypoxic environments. VEGF also plays a central role in pathological angiogenesis by inducing expression of anti-apoptotic proteins in ECs, contributing to tumor growth. Besides biochemical stimuli, mechanical cues, such as shear flow (Figure 1C), also affect angiogenesis and network morphology, as is discussed later in relation to microfluidic models.

Vessel formation *in vitro*

Our understanding of the process of angiogenesis is largely attributable to studies employing the numerous *in vivo* and *in vitro* models that are available (reviewed in [7]). However, technical issues pervade *in vivo* assays, making *in vitro* models an attractive alternative. For example, the ability to visualize neovasculature growth in animal studies is limited, as is the control over chemical, geometric and biological parameters in these models. These complexities confound the quantification from these models. Thus, *in vitro* studies including 2D scratch assays, barrier methods (Teflon stamp), chemical droplets and planar microfluidics provide a useful, albeit simplistic, alternative to study migration and morphogenetic assays of ECs. More complex culture assays, such as Transwell migration using modified Boyden chambers and the aortic ring assay, are now routine [8]. However, technical limitations persist – Transwell devices lack a realistic microenvironment, and explant models suffer from issues with reproducibility and long-term viability. Alternatively, simplistic 3D engineered models revealed important functions of single vessels under normal and pathological conditions [9], demonstrating the need to move toward 3D *in vitro* assays early on.

Many models are now designed to mimic *in vivo* geometries, enabled significantly by the use of microfluidics-based techniques. Along with ease of reproduction, cost–effectiveness and use of flexible polymers such as polydimethyl siloxane (PDMS), microfluidics offers the capability to produce well-defined micron-scale geometries and can be designed to distinguish between subtleties of chemokinetic and chemotactic effects, for example [10]. Combined with biologically derived hydrogels, an increasing number of microfluidic designs have emerged to study 3D lumen and branched networks of capillaries in one of two approaches: predefined patterning or self-assembly, both of which will be discussed in the following sections.

Networks cast or patterned in hydrogel

Patterning has been used in the development of both macro-scale single vessels and microscale vasculature. Early on, the Tien group formed perfusable vessel-like structures (75–150 μm diameter) with human umbilical vein ECs (HUVECs) or human dermal microvascular ECs seeded into the hollow region of collagen gels left by the removal of etched needles [11]. These vessels remained stable and functional for 2–3 weeks, as determined by a distinct barrier to perfusion of albumin, under flow similar to venules (1–4 Pa) and at low lumenal pressures. Moreover, HUVECs attracted neutrophil-like hu man promyelocytic leukemia (HL-60) cells, alone and in the presence of TNF-α [11]. Similar needle-based techniques, including self-assembled monolayers onto gold-sputtered rods [12], and a uniaxial layered approach [13] have since been used in combination with hydrogels to produce single perfusable vessels.

More recent patterns are employed to generate entire microvascular networks, allowing for the study of

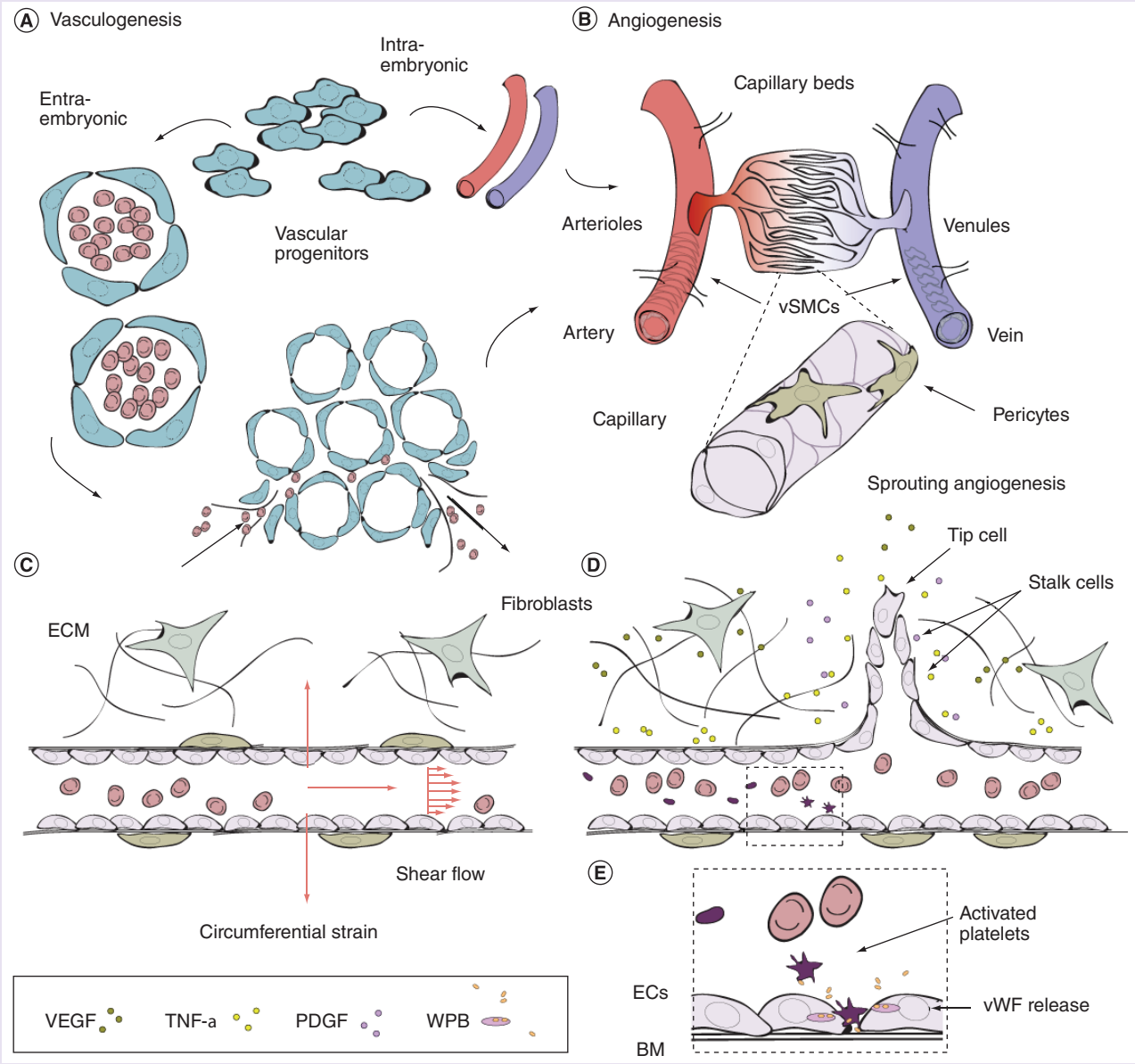

Figure 1. Vascular network formation *in vivo*. **(A)** Vascular progenitor cells directly form the dorsal aorta and cardinal vein (intra-embryonic) or coalesce into endothelial lined blood islands, which subsequently fuse into a primary plexus (extra-embryonic) and together form primary vasculature. Upon assembly, arteries and veins inosculate into smaller arterioles and venules (80–100 μm), and subsequent branching forms smaller capillaries and venules (10–15 μm). **(B)** Angiogenesis ensues and vessels mature and remodel, directed by a variety of angiogenic factors and cytokines (acidic FGF, bFGF, TGF-α), TFG-β, HGF, TNF-α, angiogenin, IL-8 and the angiopoietins [3]). **(C)** Pressure drives the perfusion of blood through capillaries, resulting in an efficient method for exchange of O_2 and small molecules across the endothelium, and larger molecules, such as drugs, delivered through the endothelium. Connection to postcapillary venules drives the inward transport of CO_2 and waste. Mechanical factors such as wall shear stress and axial strain also direct angiogenesis. **(D)** EC-secreted factors, such as TGF-β1, recruit mural cells during angiogenic remodeling. Pro-angiogenic factors are released from stromal cells such as fibroblasts, directing migration and sprouting of ECs. **(E)** Along with mural cells, and a continuously remodeling BM, ECs largely comprise the endothelium. Specialized organelles, WPBs, contained within ECs respond to various agonists (thrombin, histamine, VEGF, epinephrine, among others) by secretion of a variety of factors involved in wound healing and thrombosis. The most abundantly secreted glycoprotein is vWF. Secretion of vWF into circulating blood results in its binding to a blood-clotting factor, VIII, in its inactivated state. In the presence of thrombin, VIII is released, and vWF binds to glycoprotein Ib allowing for platelet adhesion and plug formation in sites of vascular injury.
BM: Basement membrane; EC: Endothelial cell; WPB: Weibel Palade bodies; vSMC: Vascular smooth muscle cell; vWF: von Willebrand Factor.
Concepts for Figure 1A & B are adapted with permission from [2].

highly controlled geometries of ECs under a variety of conditions, including flow (Figure 2A) [14]. Patterning is facilitated by employing soft lithography to generate molds for fabricating channels of known geometries and orientations in PDMS. Furthermore, embedding these networks into hydrogels allows *in vivo*-like degradability and remodeling of the matrix [15–17]. Combinations of PDMS stamps and jigs have resulted in complex embedded networks, where, for example, HUVECs in a collagen bed alter channel geometry in just 3 days, and result in angiogenic sprouting (Figure 2B) [15]. Stromal cells added during injection

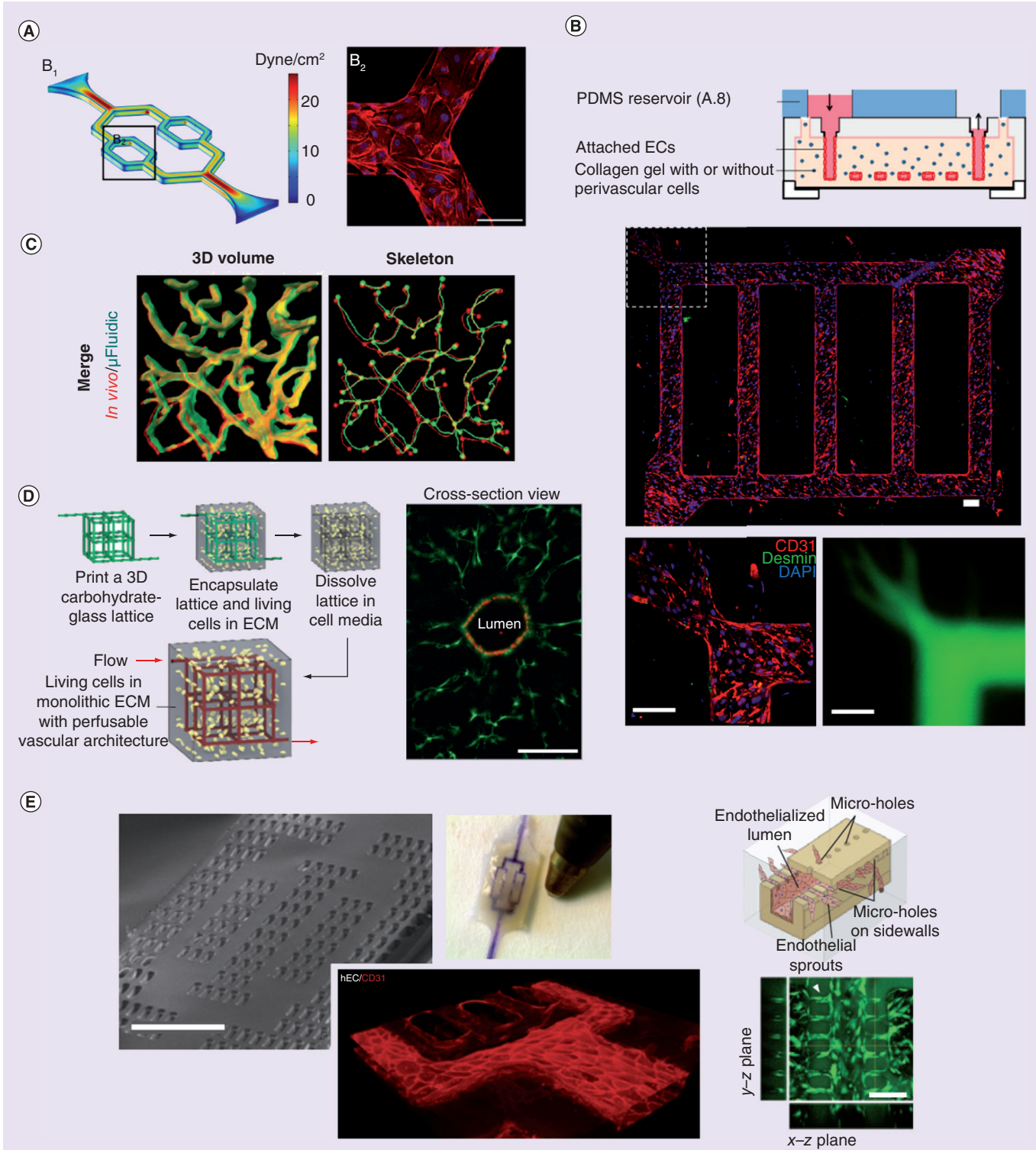

Figure 2. Examples of patterned network formation *in vitro* (see facing page). **(A)** Patterned vascular channels in polydimethyl siloxane. Low and high shear flows are simulated and examined in bifurcated channels lined with ECs. **(B)** Networks cast in hydrogel. Shown are networks of ECs lining channels in collagen embedded with pericytes (green, top and left). Pro-angiogenic factors caused pericyte localization and angiogenic sprouting into the gel. Bottom right shows the network perfused with 70 kDa dextran. **(C)** An enlarged region of cerebral cortex vasculature generated from a confocal image stack (red) was used to generate a (green) biomimetic microfluidic network by image-guided laser based degradation of PEGDA hydrogel. **(D)** Sacrificial scaffold of carbohydrate glass used as a model for vascular networks embedded in hydrogels. Right image shows a representative EC-lined channel (Human umbilical vein endothelial cell, mcherry) surrounded by mural cells (10T1/2 mouse fibroblasts, EGFP) after 9 days in culture. **(E)** Multi-layered implantable vascularized organ-on-chip, AngioChip. Shown (from left to right) is a scanning electron microscopy image of the porous scaffold, an entirely perfused chip, staining of ECs for CD31 on day 2 of culture in the device, and the sprouting of vessels through microholes.
ECM: Extracellular matrix; EC: Endothelial cell; PDMS: Polydimethyl siloxane.
(A) Adapted from [14], under a creative commons license.
(B) Adapted with permission from [15].
(C) Adapted with permission from [16] © John Wiley and Sons (2016).
(D) Adapted with permission from [17] © Macmillan Publishers Ltd: Nature Materials (2012).
(E) Adapted with permission from [18] © Macmillan Publishers Ltd: Nature Materials (2016).

of these hydrogels have also been shown to colocalize with EC channels (Figure 2B).

An alternate method for generating embedded patterns is by subtractive scaffolding (Figure 2D). Sacrificial templates of gelatin [19], sodium alginate [20] and synthetic PEG [21], have been used as scaffolding for gels of type 1 collagen and fibrin. Following removal of the scaffold, hollow channels are seeded with ECs, immediately promoting convective delivery of media and perfusate, while complementing slower diffusion processes through the hydrogel. Digitized vessels (Figure 2C) and laser-based degradation of hydrogels [16,22], as well as vascular corrosion casting [23], all produce biomimetic cast networks. One drawback of casting hydrogels is the limited control over gel alignment and distribution, as typically heterogeneous gels (natural and synthetic) are employed. Moreover, some of these systems require long-term cultures (1–2 weeks), during which cell-dependent gel degradation will occur and may present challenges with respect to observation of angiogenic growth. For a complete discussion on the use of hydrogels for tissue engineering applications, we refer the reader to the review by El-Sherbini and Yacoub [24].

Models of angiogenesis

The importance of angiogenesis is obvious in development, but also has major implications in adult wound healing and tissue regeneration. Moreover, its role in cancer is now well-known thanks to pioneers in the field such as Judah Folkman, who demonstrated avascular and vascular phases of solid tumor growth, tumor release of angiogenic factors [25,26] and anti-angiogenic factors (see [27] for a list). An entire field of research has developed around potential pro-angiogenic and anti-angiogenic therapies for the treatment of vascular diseases and cancer, respectively. For necessary high-throughput angiogenic drug testing, microfluidics models are primed to be a time- and cost-saving alternative to *in vivo* and explant models. Microfluidic-based assays examine the basic angiogenic steps including: degradation of the surrounding matrix, invasion, proliferation, morphogenic reorganization and vessel stabilization [28–31]. These processes have been studied by growing monolayers of ECs on the surface of native ECM matrix proteins, coated beads and more recently between PDMS channels.

Besides microfluidic models, hydrogel-based assays reveal important findings about the process of angiogenesis. For example, Nakatsu *et al.* used a modified version of Nehls and Drenckhahn's assay [32] by coating microcarrier beads with ECs and suspending them in fibrin gel [33]. These HUVEC-coated beads organize sprouts over 4–5 days, with tip cells extending into the gel within 2 days in the presence of skin fibroblasts [33]. From their model, exogenous VEGF, but not bFGF, is seen as sufficient for capillary formation, but not for long term (>7 days) maintenance. VEGF optimally induces sprouting at lower (2.5–5 ng/ml) not higher concentrations (15–35 ng/ml), and pro-angiogenic factors TGF-β and Ang-1 do not promote angiogenesis in the absence of fibroblasts, demonstrating multiple factors and cytokines are at play. Importantly, this work demonstrates the supportive role of stromal cells in sprouting angiogenesis, lumen formation, and vessel stabilization, which is cell-type dependent [34]. While geometrically simplistic, these models provide insight into self-directed sprouting in the presence of multiple EC sources concomitant with degradation of the surrounding matrix.

Now widespread, PDMS-based microfluidics (reviewed in [35]) allows for incorporation of 3D hydrogels in a variety of geometries, which is particularly useful for studying angiogenesis. In one example, arrays of

mixed gels connect opposing EC monolayers, resulting in tip-cell migration and lumen formation spanning gel regions in 3–4 days [36]. These gel-arrays, separated by PDMS, allow formation of multiple vessels; but at the cost of channel dimensions strongly impacting lumen formation. Alternatively, Farahat *et al.* [29] developed a microfluidic model for parallel angiogenic sprouting (similar to that in Figure 3A). Through analysis of the air–liquid interface and by exploiting the hydrophobic nature of PDMS, precisely spaced microposts facilitate confinement of the liquid gel during insertion to an inner channel. Following polymerization, media is added to the outside channels. The interface between the gel and media allows for nutrient exchange, the addition of factors either uniformly or in a gradient, and promotes self-directed sprouting [28,29,37]. Using this model, VEGF and sphingosine-1-phosphate (S1P) were shown to affect growth and directionality of angiogenic sprouts [29]. In a similar set-up, opposing EC-lined channels sprout toward one another through a collagen gel, promoted by VEGF [28]. Following anastomosis, these networks can be perfused (within several days). These rates of vessel formation are similar to *in situ* models where explants embedded in fibrinogen generate angiogenic vessels within 2–3 days [38].

Further modifications to the single-gel channel design allow for examination of the effect of growth factors, cytokines, ECM adhesion molecules and cocultures, on angiogenesis. For example, multigel systems allow for the addition of chemo-attractants on one side and control media on the other [41]. Using this method, VEGF promotes migration of human microvascular ECs (HMVECs) prior to ECs forming confluent monolayers [41]. These models, when combined with particle tracking and reflectance imaging, can be used to examine the impact of angiogenic sprouting on ECM organization. In this way, tip and stalk cells have been shown to push and pull on collagen fibers (up to ~1 μm displacement) rearranging them in an anisotropic fashion [42]. Careful *in silico* design has also allowed for VEGF to be continually perfused using source and sink reservoirs to produce a stable gradient at low flow (8 nl/min) and minimal shear (~10^{-6} Pa) [43]. Control over flow is important, as gradient direction influences vessel dilation (negative) and sprouting (positive) [28]. Growth factor gradients can also arise from cocultures. For instance, paracrine signaling of VEGF, from alginate-encapsulated fibroblasts, stimulates EC vessel formation when embedded within a gel-channel model [44]. In the same model, a combination of prolyl hydroxylase inhibitor to stabilize HIF-1α in normoxia and S1P, results in increased expression of pro-angiogenic factors in ECs, and in fibroblasts, by increased VEGF secretion [44]. These examples highlight some of the complex interactions observed in *in vitro* models.

While useful for studying angiogenesis, the models discussed do not stem from a pre-existing network. In light of this, some have induced sprouting from microvessel-like structures. For example, introduction of pro-angiogenic factors adjacent to an EC-lined vessel promotes neovessel growth into a surrounding gel [30]. Viscous fingering (infiltration) of media within gel-lined constructs can be used to generate relatively large (~250 μm) endothelial-lined lumens [45,46]. Models employing these vessel-like structures demonstrate VEGF-induced angiogenic sprouting; however, the PDMS mold surrounding the embedded gels influences the morphology of endothelial-lined lumens [46], which are essentially patterned networks. Angiogenic sprouting has also been shown from the ends of vessel-like structures of ECs derived from induced pluripotent stem cells (iPSC; iPSC-ECs) in 3D Matrigel constructs [47]. Combining self-assembled and patterned networks may be one way to promote macro and micro network connectivity, a necessary consideration for development of engineered tissues.

Models of vasculogenesis

The utility of microfluidic techniques is unparalleled for studying vasculogenesis, as demonstrated by recent models [48,49]. *In vitro* vasculogenesis typically relies on careful mixing of ECs with collagen or fibrin gels, which subsequently self-assemble into networks (Figure 3A). For example, by encapsulating stromal cells in the outer gels of a 3-gel system, HUVECs (in the middle gel region) begin forming networks within 24 h [48]. systems, such as these, result in patent lumens in 4 days, as confirmed by flow of fluorophores or fluorescent beads. These networks quickly regress in the absence of fibroblasts [48], demonstrating the usefulness of parallel gel channels for examining paracrine signaling. Variants to straight gel regions, for example, diamond-shaped, have also been used to generate nearly identical mechanical environments of perfusable networks (Figure 3B) [40,50]. In models such as these, vasculogenesis occurs across approximately 1 mm [48,50] length scales, where prevascularization is necessary *in vivo*. The width of cell-seeded gel regions dictates the diffusion rate of secreted factors from adjacent channels (approximately several hours for 1 mm, depending on the diffusivity of the molecule), and must be considered in the design process, particularly in the absence of applied flow. Microfluidic models can, however, be designed to incorporate flow in order to drive angiogenesis [28,31], vasculogenesis [40] or encourage directional growth by alternating flow in channel arrays [50]. Single layer soft-lithography is limited to approximately 100 μm, making these

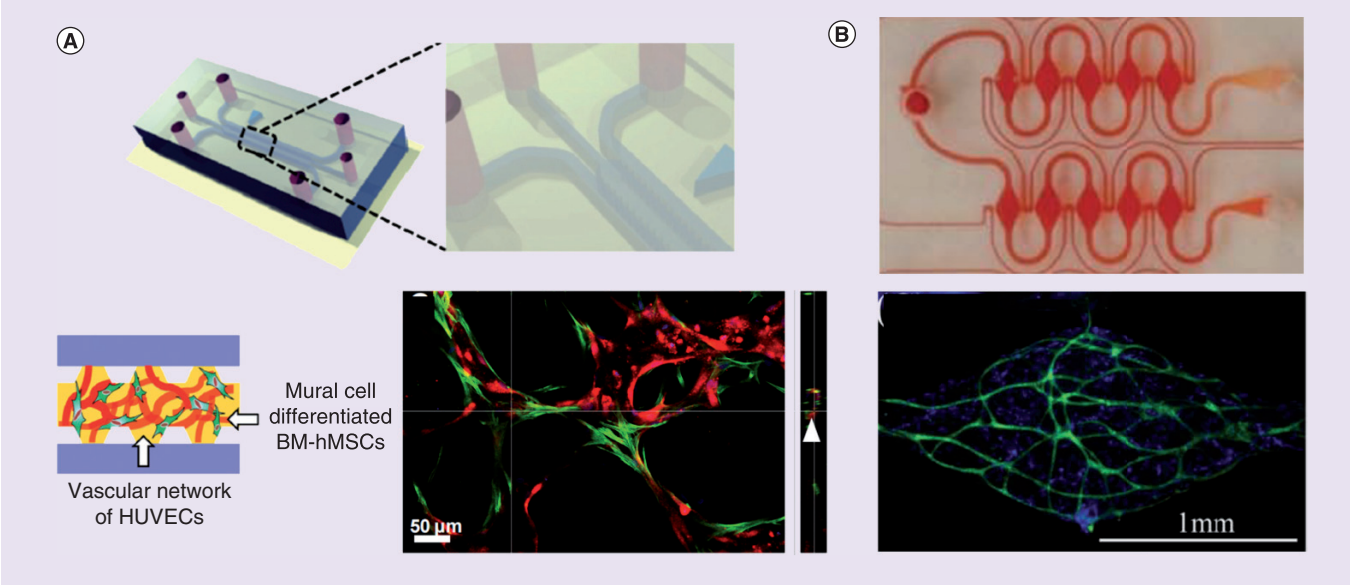

Figure 3. Examples of self-assembled *in vitro* networks. (A) A single-gel channel model with posts. Bottom shows a self-assembled network of HUVEC (green) and mural cells - bone marrow derived hMSCs (red) after 1-week culture with VEGF + Ang-1 supplemented media. **(B)** Self-assembled networks of (top) perfused microtissue array, with vascular networks formed by normal human lung fibroblasts and endothelial cells (CD31, green; nuclei, blue) in fibrin gel (bottom shows one region from the top array).
BM: Basement membrane; hMSC: Human mesenchymal stem cell; HUVEC: Human umbilical vein endothelial cell.
(A) Adapted with permission from [39] © The Royal Society of Chemistry.
(B) Adapted with permission from [40] © The Royal Society of Chemistry.

microfluidic designs relatively planar. Generating thick gel-models is achievable by other means (such as 3D printing), but mimicking tissue-like thickness comes at the cost of requiring larger numbers of cells, and difficulties with imaging thick samples.

The ability to generate perfusable microvascular networks in a relatively short period of time has allowed for the observation of physiologically relevant events in real-time. For example, a double-gel device, with HUVECs cultured in one channel and normal human lung fibroblasts (nHLFs) in the other, is perfused by day 4 and allows for observation of trans-endothelial migration of tumor cells [51]. Observations of tumor cell trans-endothelial migration demonstrates that tumor cells which are trapped in narrow vessels extravasate more readily than adhered, nontrapped, cells (~50% vs ~10%) [51]. Moreover, the effects of inflammatory cytokines such as TNF-α introduced into the media reservoir increase microvessel permeability and extravasation of MDA-MB-321 (epithelial breast cancer) cells [51]. In another example, EC-lined channels are combined with self-directed vasculogenesis in a gel-region to generate a perfusable artery and vein anastomosed with a microvascular network [52]. A hydrostatic pressure gradient applied to the system mimics physiological flows, likely resulting in a more functional EC barrier to transport. Major limitations of many of the models discussed are the lack of appropriate stromal cells and the use of PDMS to form the channels, which does not allow for vasodilation or constriction of lined channels and adsorbs small, hydrophobic molecules. As well, microvessels formed *in vitro* tend to be larger (up to 50 µm), in comparison to *in vivo* capillaries (<10 µm).

Mimicking *in vivo* conditions *in vitro*

In order to mimic *in vivo* conditions in health or disease, characterization of form and function of formed microvessels is necessary. Number and length of branches, patent area and average vessel diameter, are often used to distinguish network quality [40,48,49]; however, many factors alter morphology. Cell density, for example, has a significant effect on branching, with decreasing branch diameter and length a result of increased concentration [48]. When cocultured with fibroblasts, pro-angiogenic factors (VEGF and S1P) promote network regression. Vessel diameter and length reduce in size while networks remain intact, closely resembling those seen *in vivo* [48]. Immunofluorescence is commonly used to indicate endothelial phenotype and connectivity of networks, namely by expression of CD31 and vascular endothelial (VE)-cadherin, respectively [53]. Formation of tight junction proteins, indicated by zonula occludins-1 (ZO-1) [36] and expression of basement membrane (BM) proteins (laminin and collagen IV), and EC polarity, all indicate vessel maturity [49].

Besides connectivity, EC function is demonstrated by a normal thrombotic response during quiescence and upon exposure to inflammatory mediators. As an early example, localization of vWF and release of prostacyclin (a potent inhibitor of platelet aggregation) has been demonstrated from single-vessels in collagen [9]. ATP has also been used to induce a transient increase in Ca^{2+}, resulting in increased nitrous oxide (NO) production in EC-lined microvessels [14], both of which are directly related to vessel permeability [54]. Moreover, adhesion of leukocytes, platelet aggregation and upregulation of adhesion molecules, such as intercellular adhesion molecule 1 and melanoma cell adhesion molecule have been shown in response to inflammatory cytokines such as TNF-α and IL-1α in multichannel devices [47,49]. Perfusion with whole blood, has also demonstrated antithrombotic properties of *in vitro* networks [15]. In the same model, further stimulation of protein kinase C led to a movement of von Willebrand factor from cytoplasmic WPBs to the surface of ECs, where they bound platelets irreversibly (as depicted in Figure 1E) [15]. Often, multiple methods are used to assess function of *in vitro* networks; however, demonstrating a barrier to diffusion and measurements of permeability are essential.

Permeability as a measure of microvessel function

Transport of macromolecules across the endothelium is a primary function of *in vivo* microvasculature, where strong barrier function is the result of tight junctions, the glycocalyx, BM, as well as mural cell interactions (Figure 4A). Various modifications to the Miles assay [55], including the use of fluorescently labeled albumin, have been employed to examine permeability of microvessels *in vivo*. By extension of these densitometry techniques, Huxley, Curry and Adamson developed an *in situ* method for measurement of diffusional permeability in frog mesenteric capillaries [56]. Briefly, following introduction of a fluorescent perfusate to the lumen of a vessel, intensity is measured over time. This method takes advantage of a linear relation between fluorescence intensity and fluorophore concentration. Convective transport across the capillary wall is neglected in this model, resulting in an overestimated effective permeability (P_e).

Despite distinct differences with the microenvironment (lack of a pressure gradient and vasoconstriction/dilation), measurements of permeability are often used to assess *in vitro* formed networks [59]. For example, impedance-based platforms have been used in the presence of disruptors of barrier function (10× thrombin solution) [47], and transendothelial electrical resistance is often measured in Transwell devices [45]. Due to its relative ease of implementation, the *in situ* method of Huxley, Curry and Adamson has also been adopted for measurement of P_e in microvessels formed in microfluidic devices (Figure 4B–D) [11,49,51–52,60]. While measurements of hydraulic permeability are similar, reports of permeability to solutes *in vitro* are often significantly higher (by as much as two orders of magnitude) than *in vivo* [57] (see Table 1 for values from a variety of models). These differences result from changes in phenotype brought about during cell culture, noted differences in the *in vitro* endothelial barrier (possible lack of a functional glycocalyx, basal lamina and surrounding pericytes), and the varied response to inflammatory agents resulting from prior exposure to inflammation or injury (reviewed in [58]). Moreover, perfusion methods employed *in vitro* often neglect contributions due to convection (as in the Huxley method). While simpler, its consideration is necessary for efficient perfusion, and is more biologically relevant. Accounting for both diffusion and convection is achievable by measuring diffusivity of solutes across an acellular matrix, as in [61], and using mass transfer to determine P across an endothelium of known geometry, as in the patterned collagen networks of Zheng *et al.* [15]. However, this type of measurement becomes increasingly difficult to assess in self-directed networks, where geometries are variable and include many intersecting network branches (see Figure 4B & C).

Microfluidic models have been useful in demonstrating the effect of angiogenic factors on transendothelial permeability. For example, VEGF, which impairs cell–cell adhesions (Figure 4A), and a lack of S1P, which is known to stabilize the actin band, both result in increased permeability to solutes. Exposure to angiogenic growth media increased permeability by an order of magnitude following continuous perfusion for 7 days in an embedded gel-channel model (Figure 2B), a result circumvented by coculture with pericytes [15]. Permeability of vascular ECs is also known to be affected by cAMP [60], which also increases the barrier function of lymphatic ECs (LECs) [26]. Besides factors and cytokines, mechanics also plays a role in regulating solute permeability. For example, single EC-lined lumen formed in a collagen gel, demonstrate improved barrier function with increasing flow rates and shear stress [65]. Interestingly, combining high flow rates with dibutryl cAMP (known to increase intracellular levels) did not result in a further increase in permeability, rather mitotic rate was decreased, prolonging the longevity of the microvessels. Factors including cell phenotype, perfusion conditions, matrix material and density, as well as vessel geometry, can have a significant effect on permeability. While easy to measure

in monolayers and single-vessel geometries, measurements in patterned and self-assembled networks of heterogeneous geometry are more challenging.

Microenvironment control

Microfluidic techniques offer exceptional control over the designed microenvironment, which is necessary to generate realistic vascular networks *in vitro*. However, the choice of embedded hydrogel will influence the formation of microvascular networks and impacts the ability to replicate *in vivo*-like processes of degradation, sprouting and neovascularization of *in vitro* networks. For instance, stiffer gels produce more *in vivo*-like morphology, generate small diameter lumens (20–30 μm diameter) and restrict EC migration [41]. Natural hydrogels such as collagen and fibrin are often used and have certain advantages. For example, the mechanical properties of collagen can be easily tuned by gelling at different temperatures or pH, as well as by altering protein concentration. However, collagen can also detach from PDMS, likely a result of low extensibility and gel contraction by cells over time. For this

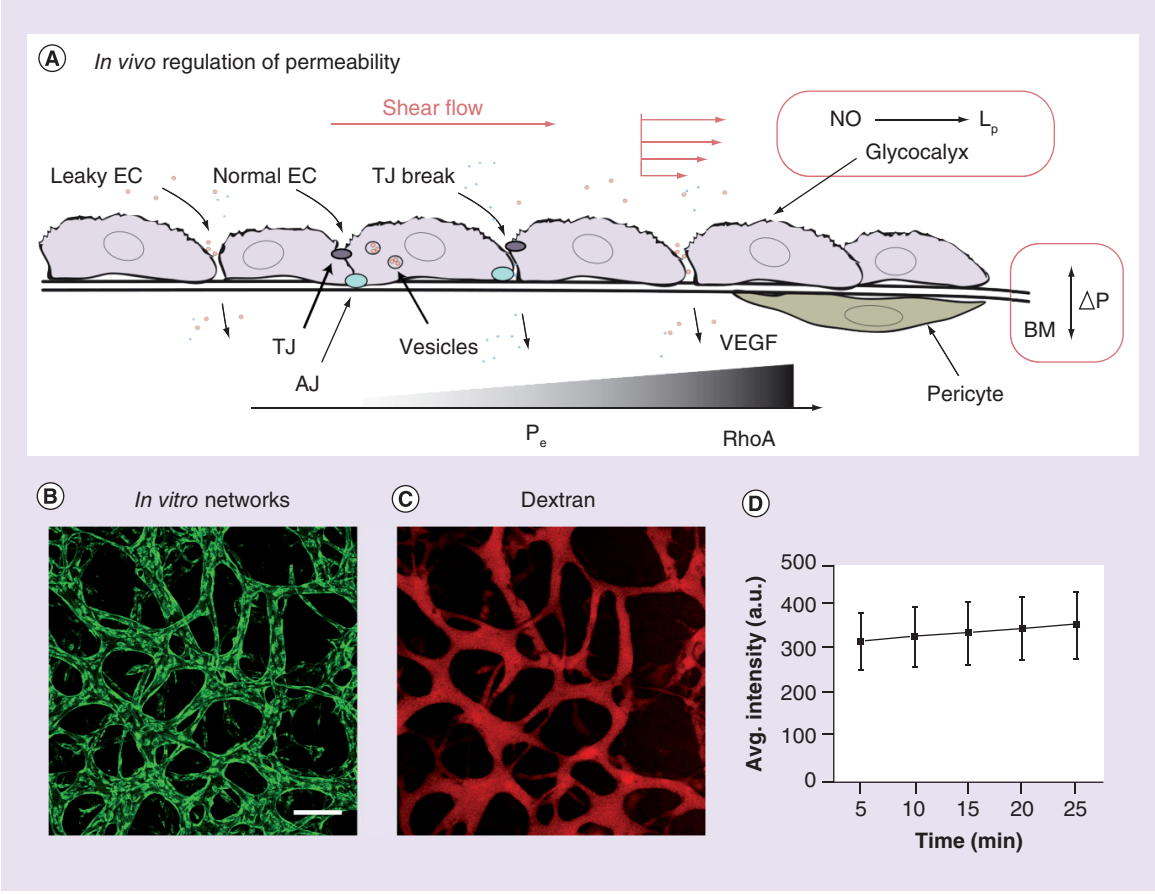

Figure 4. Permeability is an important indicator of network function *in vivo* and *in vitro*. **(A)** Schematic diagram demonstrating the three-pore model, including normal ECs, TJ breaks and leaky AJs, as reviewed in [57]. Besides vesicular transport, shear flow and regulated pressure differences across the BM are necessary to maintain the EC intercellular barrier to flux of small solutes and large macromolecules. Leaky junctions result from low flow as well as high shear forces; regulated by complex expression of junctional proteins such as vascular endothelial-cadherin and occludin. ECs release nitrous oxide in response to shear, which increases L_P, but not P_e to solutes. Increased VEGF expression and changes in the cortical actin network (via RhoA) are known to correspond with an increased P_e. The glycocalyx plays a role in mechanostransduction of shear as well as forms a selective barrier to plasma proteins, breaks in which result in leaky ECs [58]. **(B–D)** Author's unpublished results. **(B)** Self-assembled vascular network of human umbilical vein endothelial cells (green) after 7 days in culture with normal human lung fibroblasts in fibrin in a single-gel microfluidic model (similar to that in Figure 3A). Scale bar is 200 μm. **(C)** Single vessel, or network, P_e can be measured by perfusion with fluorescent tracers. Shown here is the network in **(B)** perfused with 70 kDa fluorescent Dextran. **(D)** Shown is a linear increase in measured fluorescence intensity of extracellular perfusate over time. Shown are representative values (mean + standard mean error) from regions surrounding the perfused network.
AJ: Adherens junction; Avg.: Average; BM: Basement membrane; EC: Endothelial cell; L_P: Hydraulic permeability; NO: Nitrous oxide; P_e: Effective permeability (to solutes); TJ: Tight junction.

Table 1. Comparison of permeability measurements made using *in vivo*, *in situ* and *in vitro* models with varied perfusate.

Perfusate	Cell type	System	Permeability (P_e cm/s)	Culture (days)	Ref.
BSA (66.5 kDa)	Granulation	*In vivo*	~10^{-7}–10^{-8}, capillaries	N/A	[62]
		Rat	~10^{-8}–10^{-7}, venules		
150 kDa dextran	VX2 carcinoma	Rabbit (ear)	~10^{-8}, normal	~40	[63]
			~10^{-7}, tumor		
70 kDa dextran	BBB	Rat	15.0 × 10^{-8}, venules	7–10	[64]
14.2 kDa α-lactalbumin	Frog mesentary	*In situ*	1.9 × 10^{-6}, capillary (8 cm H_2O)	N/A	[56]
		Vessel	3.0 × 10^{-6}, capillary (8 cm H_2O)		
			2.2 × 10^{-6}, capillary (0 drag)		
BSA	HDMEC	*In vitro*	5.5 × 10^{-6}, venule-like	2	[11]
		Single vessel			
BSA	LEC	*In vitro*	1.4 × 10^{-6}, †1.1 × 10^{-7}	3	[60]
10 kDa dextran	BEC	Single vessel	1.7 × 10^{-6}, †3.8 × 10^{-7}		
			†db-cAMP + Ro-20-1724		
20 kDa dextran	HUVEC	*In vitro*	4.05 × 10^{-5}	3–4	[20]
70 kDa dextran		Cast in hydrogel	0.66 × 10^{-5}		
70 kDa dextran			4.1 × 10^{-6}	14	[15]
332 Da fluorescein			7.0 × 10^{-6}		
70 kDa dextran		*In vitro*			
	HUVEC + nHLF	3-gel system	1.70 × 10^{-6}	4–5	[49]
	HUVEC + nHLF	2-gel system	8.92 × 10^{-7}	4	[51]
BSA (FITC-labeled)	HUVEC	ELL	4.73 × 10^{-6}	2	[46]
3 kDa dextran	HBMVECs	*In vitro*			
Continuous perfusion	+ pericytes and	BBB	4 × 10^{-6}	5	[45]
	astrocytes	Single vessel	2–3 × 10^{-6}		

†Represents P_e under treated conditions.
BBB: Blood–brain barrier; BEC: Bovine endothelial cell; cAMP: Cyclic adenosine monophosphate; ELL: Endothelial-lined lumen; FITC: Fluorescein isothiocyanate; HBMVEC: Human brain microvascular endothelial cell; HDMEC: Human dermal microvascular endothelial cell; HUVEC: Human umbilical vein endothelial cell; LEC: Lymphatic endothelial cell; N/A: Not applicable; nHLF: Normal human lung fibroblast.

reason, co-gels of varying percentages of collagen and fibrin are often used to mediate mechanical properties toward amenable gels for angiogenic/vasculogenic assays [66]. Strain stiffening properties of fibrin (occurs at larger strains and higher yield strength than collagen) make it an ideal gel for the formation of networks of ECs, particularly HUVECs [67]. Alternatives to collagen and fibrin, such as synthetic ECM proteins are also commonly employed; an overview can be found in the review by Kannan *et al.* [68].

Besides hydrogels, consideration of EC phenotype is crucial for network formation. There are marked differences between physiology (fenestrated vs sinusoidal) and functionality (permeability, and specific factors and receptors) of endothelium between, for example, brain and different regions within the lymphatic and circulatory systems. Well-established gene expression and physiology of HUVECs has resulted from their widespread use; however, organ-specific cell types should be considered, and are likely essential for certain applications. Nakatsu *et al.* demonstrated similarities in sprouting vessels between HUVECs and lung microvascular ECs in the presence of skin fibroblasts, but no vessel formation occurred using bovine aortic ECs [33]. Whether mature or pluripotent cells are more suitable for therapeutic assays, or tissue engineering, also remains an open question. HUVECs have shown success with network formation; however, their proliferation is limited in the absence of pro-angiogenic factors [69]. Acting as a precursor to both ECs (initiated by VEGF) and mural cells (induced by PDGF-BB), embryonic stem cells [70], iPSCs [47] or other vascular precursors may provide a useful alternative to HUVECs.

How EC networks react with mural cells is an area of intense investigation. Mural cells, including pericytes, regulate vascular growth and maintenance *in vivo* [71], and sustain vascular lumen formation and patency *in vitro* [33–34,72]. The inclusion of stromal cells into microfluidic vascular models has been shown to not

only stabilize, but also organize ECs into more mature, smaller networks. Fibroblasts, in particular, direct network formation by synthesis and maintenance of the ECM, and secretion of a variety of angiogenic growth factors and proteins in response to wound healing and during tumor growth. Fibroblast-conditioned medium promotes EC sprouting and lumen formation, but at reduced levels compared with cocultures [34]. Coculture with encapsulated fibroblasts (to prevent juxtacrine signaling) demonstrated that soluble factors were sufficient for angiogenic sprouting in a 3-gel channel model [44]. Moreover, HUVECs have been shown to attract pericytes in gel-channel models [49]. As *in vivo*, pericytes align next to lumens [73] and tend to contract the gel over time. Cocultures have complicated effects on the growth of networks. A high cell density, for instance, might be necessary to efficiently form networks, but may cause depletion of oxygen and nutrients from the culture medium. Moreover cell-type dependencies are noted, as in an angiogenic model, where U87MG (human primary glioblastoma) attracted HMVEC cells faster than MTLn3 (rat mammary cancer cell line), and 10T ½ (SMCs) suppressed migration [41]. Cocultures of ECs and perivascular cells embedded in synthetic scaffolds have also been successfully implanted *in vivo* [74]. Successful perfusion and long-term survival of these tissue-like structures demonstrates the relevance of cocultures in regenerative medicine.

Mechanical control

Blood flow through patent vessels results in shear forces tangential to vessel walls as well as pressure differences across them. Patterns of flow are complicated by bifurcations leading to regions of disturbed flow in large arteries, which are susceptible to atherosclerosis and other inflammatory issues. Mechanical cues such as these (see examples in Table 2) have pronounced morphologic and functional effects on ECs and microvessels. Therefore, exposing patent microvessels *in vitro* to physiologically relevant forces is crucial for understanding vascular growth, function, and maintenance.

Shear flow *in vivo* is known to alter cell–cell contacts, and lead to decreased permeability of networks (Figure 4A). The physiological effects of shear flow involve a complex of mechanosensitive components including VE-cadherin, PECAM-1 and VEGFR2 [81,82], all well-known to direct network morphology. The effects of shear flow have been examined both in 2D and in 3D microfluidic models. For example, an impinging flow device has shown HMVECs re-orient above a critical threshold [83], in contrast to alignment of bovine aortic ECs [75], and HUVECs [84]. Elongation of iPSC-ECs parallel to shear flow has also been demonstrated in a 2D flow chamber and in the direction of shear in vessels within 3D Matrigel [47]. Microfluidic models have also demonstrated EC alignment in the direction of applied physiologic shear flow [20,49]. Shear flow can be readily examined using both patterned and self-assembled models of microvasculature. Addition of convective fluid flow is relatively simple in patterned microfluidic networks, whereas fluid flow in parallel gel-channels (or other geometries) is produced by bulk perfusion across the gel region containing vessels [28,37,50]. In these parallel channel models, steady state flow can be generated using large media reservoirs in order to provide a stable pressure drop across the gel region. Estimates of shear stress at the channel are possible given known geometries and the viscosity of the media (as in [14,59]). Using methods such as these, physiologic levels of flow (Table 2) and complicated flow patterns (bifurcated regions) can be generated and systematically characterized *in vitro*.

Other types of flow can also be generated in microfluidic models. For instance, convective flow through media channels can result in pressure gradients and interstitial flow across the gel region, as was demonstrated in the single gel channel device of Song and

Table 2. Vessels experience various magnitudes of mechanical forces *in vivo*.

Mechanical force	Magnitude, condition	Localization	Ref.
Wall shear stress	1.5–2 Pa, normal flow >4 Pa, impinging flow 0.1–1 Pa	Arterial segments Birfurcations Venules, arterioles	[75]
Circumferential stress	2–18%, change in mean diameter (during oscillations)	Arteries (varies on locale)	[76]
Transmural Pressure	14 mmHg, at rest 30 mmHg, during exercise 100 mmHg (maximal)	Pulmonary artery Mammary artery	[77] [78]
Axial strain Axial stress	40–60% (from tethers to connective tissue) 100–200 kPa	Arterial vessels	[79] [80]

Munn [28]. Interstitial flow has been shown to induce angiogenic sprouting in a directional manner, with basal to apical flow resulting in Src-dependent of VE-cadherin and remodeling of the actin cytoskeleton [31]. Interstitial flow along with pro-lymphangiogenic factors has also recently been shown to promote lymphatic sprouting in a 3D gel-channel model [85]. A major advantage of microfluidics is that device design, with the help of finite element analysis, can be tailored for precise application of shear stresses and transmural pressures. Using tapered vessel geometries, Price *et al.* demonstrate high shear and positive transmural pressure must exist to maintain tight connections and a stable vessel phenotype of BECs in collagen [65]. In their model, increased fluid flow dilates vessels, but strain is negligible – shear is the main driver of vessel permeability. Interestingly, when high flow rates are combined with cAMP, which alone causes increased permeability [60], there is no further increase in P_e. Instead, selectivity, a reduced proliferation and longevity of vessels are demonstrated [65]. These examples demonstrate the importance of characterization of vessel networks under various mechanical flow regimes in more relevant microenvironments (EC subtype and in 2D vs 3D), made possible using microfluidic devices.

Circumferential stretch, associated with hypertension, has been hypothesized to contribute to inflammatory signaling in vascular networks. Stretch-induced exocytosis of WBPs, from HUVEC and human arterial and venous ECs, results from increased VEGFR2 phosphorylation [86]. With implications in vascular inflammation and thrombosis, it is quite clear, that this mechanical signal cannot be overlooked. Reports on the mechanical influence of stretch in 2D cell cultures has been well documented (reviewed in [87]); however, fewer reports in 3D exist. A recent study by Rosenfeld *et al.* demonstrates static tensile forces alone can direct vessel growth [53]. ECs and fibroblasts cocultured in a standalone fibrin gel experienced static tension (measured by micropost deflection) due to cell contraction and gel shrinkage. Vessels formed parallel to the orientation of static stretch, but aligned diagonally to the axis of applied cyclic stretch. Interestingly, alignment of microvessels in this way may help initiate anastomosis *in vivo*, as the authors demonstrated in rats [53]. Others have also demonstrated negative effects of shear flow and cyclic stretch on adhesion of tumor cells in an EC-lined vascular model [88]. Using computational tools [40], stretch and flow patterns can be predicted in more complex geometries, such as bifurcations. Stimulating cells with other tissue-mimetic environmental cues (strain, hydrostatic, osmotic pressure) will be important for studying complex processes such as leukocyte and platelet adhesion in the future.

Challenges in 3D

Microfluidic vascular networks have provided a wealth of information regarding EC behavior in controlled 3D microenvironments; however, interpretation must be considered in relation to native vasculature. For example, organization of endothelium *in vivo* depends on surrounding microenvironment and tissues, as seen with vessels aligned parallel to muscle, radially in the retina and highly branched in organs such as the lungs, liver and kidneys. The hydrogel and geometries used in patterned networks certainly influence angiogenic growth, as seen by distinct differences between self-assembled network morphologies [41]. Angiogenesis requires substantial ECM remodeling and is also affected by parenchymal cells. The extent to which environmental cues (such as angiogenic factors) affect vessel morphology and permeability is difficult to quantify even in simple systems. Moreover, cell-seeding densities, hydrogel distributions and CO_2 levels inside dense networks, are difficult to measure or control. Even systemic factors, such as controlling flow during media changes [50], can have an effect on network morphology and function. While cell phenotype, geometry and application of physiological conditions should all be considered in the development of more realistic networks, it may become increasingly difficult to single-out contributors and mechanisms behind changes in microvasculature structure and function.

Organs-on-a-chip

Organ-on-a-chip devices hold the promise of generating models suitable for study of tissue growth, function and disease, as well as drug testing, and development. At their simplest, these models include single-cell types in active microenvironments (ECs, hepatocytes, and so on); however, more complex tissue interfaces such as human alveolar–capillary [89], blood–brain barrier [90] and vascularized solid tumors [91], among many others models (reviewed in [92]) have been generated with the inclusion of porous membranes, cocultures and physiologically relevant dynamics. Proposed as a step closer to more realistic drug testing platforms, recent models aim to produce multiple organs on the same chip. As an example, dermal biopsies and artificial hepatic tissue were cocultured on the same chip and were shown to maintain viability over long-term culture (14 days exposed to continuous flow, and 28 days when shielded from flow). Albumin secreted by the hepatic tissue was absorbed by the skin tissue, demonstrating microtissue functionality and crosstalk [93]. Besides drug testing, microfluidic techniques have been used to fabricate implantable pre-seeded devices. AngioChip [18], by Radisic's group (Figure 2G), demonstrates an immediately perfusable millimeter scale vascularized tissue

model. This multilayered vascularized device can be tailored, as was shown, to meet tissue-specific mechanical needs of hepatic and cardiac tissue [18]. While these techniques are a step toward implantable vascularized tissues, issues with scaling-up must still be considered, as implants such as these leave little room for autologous vessels and mural cells. Moreover, limitations of engineered tissue viability (maintained by constant perfusion in bioreactors), and the initial cell-seeding density (on the order of millions for hepatic and cardiac tissue models) must be addressed before complex hierarchical vascular networks can be reliably produced.

Microfluidic organ-on-chip models overcome many prior limitations of earlier 2D assays by providing highly regulated spatial and temporal control over cell patterning, chemical gradients and mechanical stimuli, such as flow. Bhatia and Ingber suggest that an alternative to PDMS and a universal blood substitute will be necessary before *in vitro* microfluidic models completely replace animal models [92]. Integration with on-chip sensors and multi-organ systems are the next step toward human-on-a-chip models. These models have the potential to reduce or even replace animal drug testing, and lead to significant advances in personalized medicine when combined with iPSCs.

Toward vascularized tissues

Two broad techniques have been described as dominant strategies for generating vascularized *in vitro* tissues: engineered scaffolds and naturally formed, cell-based strategies. Scaffold-based strategies include naturally derived and synthetically generated tube-like structures, while cell-based strategies rely on endothelial angiogenesis and vasculogenesis to form perfusable networks (see [68] for a comprehensive overview of approaches for generating vascularized tissues). While the advantages of PDMS (inexpensive, inert, permeable to gas, flexible and optically transparent) make it ideal for fabricating microfluidic devices, adsorption of small molecules and transient mechanical properties makes it ineffective for long-term cultures, drug studies and tissue engineering (reviewed in [94]). To overcome these limitations, synthetic polymers, such as PLLA and PLGA [74], poly(glycerol) sebacate [95] and PEG [96], which are tunable and degradable, are gaining traction as porous scaffolds that allow for nutrient exchange while providing implantable tissues with necessary structural support. Cell seeding of degradable gels has been used in clinical applications of tissue engineering for bone, cartilage [97], skin and large blood vessels. Microfluidic approaches have recently been combined with synthetic polymers, as in the recent AngioChip design which used a synthetic biodegradable (~5 weeks *in vivo*) polymer, poly(octamethylene maleate (anhydride) citrate [18]. While promising for development of vascularized implantable devices, organ-specific degradation times of these polymers must first be addressed.

As with any scaffold, including those generated by decellularized tissue, electro-spinning and more recently bio-printing, the major issue faced is cell perfusion. The trend for developing vascularized tissue is moving toward the use of more than one technique. For example, bioprinting of a sacrificial lattice of carbohydrate glass generates perfusable lumen embedded in a variety of hydrogels (Figure 2D) [17]. This technique provides a rapid way to generate patterned vascular structures that are immediately perfusable. However, only large diameter lumens can currently be formed (a limitation of bio-printer nozzle) and the tissue unit still lacks *in vivo* cell densities (10–500 M/ml [17]). As an alternative to template dissolution, 3D-printed agarose can be used to form a removable template for gel-embedded vascular networks [98]. Simple vessel geometries are required to allow removal of agarose fibers by extraction from the surrounding gel. Current 3D printing techniques demonstrate the ability to print multiple cell-laden bio-inks simultaneously [99]. The emerging field of 3D printing for producing embedded vascular networks has the potential to shed light on complex interactions between ECs and pericytes in highly relevant geometries. Moreover, physiologically relevant patterns, potentially produced by these methods (see Kinstlinger and Miller [100] for a review on 3D printed vascular models), will ultimately be required to produce thick engineered tissues. Patterned vascular channels formed in malleable hydrogels have the potential for further development into prevascularized tissues necessary for highly metabolic, high cell density organs such as the liver and heart, where perfusion and antithrombotic functionality will be necessary immediately upon implantation.

Conclusion

Recent advances in microfluidic device design and fabrication methods allows for the development of complex *in vitro* models of vascular networks in hydrogels. In-depth analyses of angiogenic and vasculogenic processes are now widely studied on-chip. Through a variety of examples, we show that these models are advantageous over *in vivo* models for direct analysis of altered morphology and function (ie., permeability to small solutes) of microvessels. Moreover, mechanical cues, such as shear flow and strain, are replicated in more complex microfluidic designs, which we recommend as necessary to more closely mimic native vasculature. Insight gained from these models is vital towards our understanding of vascular development and remodeling. Importantly, microfluidics has led

to novel organ-on-chip devices which will play a large role in drug testing, and in generating prevascularized engineered tissues necessary for regenerative therapies.

Future perspective

Microfluidic models provide a relatively facile means for development of patterned and self-assembled microvascular networks. Tight control over geometry and the microenvironment makes microfluidic devices, when combined with hydrogels, ideal for investigating microvessel function and pathology. In this bottom-up approach to network development, morphology and functionality of the endothelium can be assessed as individual parameters are tuned. Through recent examples, we show that measurements of vessel permeability to small and large molecules and a functional response to inflammatory conditions are essential for network assessment. While VEGF is predominant, a myriad of factors and proteins, parenchymal cell interactions, as well as mechanical stimuli are all involved in regulating pro- and anti-angiogenic pathways. Distinguishing between the effects of multiple cues on vascular function remains a significant challenge, particularly as models become more complex. We propose that future microfluidic models must certainly include relevant cell phenotypes, especially pericytes and stromal cells, and degradable hydrogels. Moreover, complex dynamics, such as vasodilation and constriction of larger vessels and relevant shear flow through microvessel networks, have yet to be replicated *in vitro*. Bridging the gap between larger vessels and the microvasculature must also be addressed in order to integrate with tissue and organ-specific models, and ultimately for generating pre-vascularized tissue.

To date, a number of vascular as well as organ-on-chip models have been developed using microfluidic techniques in combination with hydrogels. These models provide valuable insight into the function and pathology of organotypic vasculature by mimicking physiologic conditions (e.g., shear and pulsatile fluid flow, cyclic stretch, hypoxia and exposure to thrombotic agents). Organ-mimicking models have the potential for use in drug testing and development; however, certain limitations must first be overcome. Opportunities remain for the development of methods to sustain culture of *in vivo*-relevant cell densities, and with multiple interacting cell types. In addition, device materials which are non-reactive (as opposed to PDMS), integrate well with natural ECM proteins, and allow for long-term stability, are crucial for drug testing applications. Moreover, integration of functional vascular and lymphatic networks will be necessary for reproducing realistic organ-on-chip systems. With these limitations met, the goal of one day replacing animal models and eliminating major metabolic and heterotypic differences that confound drug testing can be achieved.

The strategy of preseeding cells into biodegradable porous scaffolds has also demonstrated recent success with implantation of prevascularized tissues in

Executive summary

Microvessels formed by patterned channels *in vitro*

- Perfusable vessels are generated within 4–5 days by seeding and lining channels with endothelial cells (ECs).
- Combined with simulations, effects of shear flow can be characterized in patterned networks of controlled geometries.
- By use of sacrificial molds, patterned networks are cast in hydrogels and allow for coculture with pericytes and stromal cells as well as degradation and angiogenic sprouting within the surrounding extracellular matrix.
- New methods, such as laser ablation of hydrogels, provide microscale channels with *in vivo*-like geometries.

Microvessels self-assembled in hydrogels

- Single or multi-gel channels embedded with ECs and stromal cells self-assemble into perfusable networks within 4–7 days.
- Gel-channel devices can be used to control ensemble geometry, biochemical and mechanical cues.
- Using these models, pro-angiogenic factors as well as inflammatory mediators have been introduced to elicit changes in network growth rates and morphology and examine EC functionality, particularly permeability to solutes.

Mimicking *in vivo* conditions *in vitro*

- EC connectivity and morphology, as well as microvessel response to inflammation and measurements of permeability can be used to assess network maturity, functionality and long-term stability.
- Cell phenotype and relevant stromal cells, as well as other environmental factors, need to be considered when generating perfusable tissue-specific vascular networks.

Toward vascularized tissues

- Prevascularized models may provide an immediately perfusable solution for engineered thick tissues.
- Biocompatibility of these systems is still reliant upon culture with appropriate cells and use of porous degradable scaffolding.

animals. By capitalizing on the resolution and patterning of soft-lithography techniques, and with the use of sacrificial molds or degradable polymers, it is possible to create sufficiently porous scaffolds necessary to support embedded hydrogels. These scaffolds enable the generation of thick engineered tissues by stacking embedded hydrogel layers. Development of biocompatible and degradable scaffold materials that promote the growth of microvasculature will be the ultimate challenge toward implantable vascularized tissues. With the use of relevant cell phenotypes, such as iPSC-ECs, complex models generated using microfluidic techniques have the potential for providing valuable insights into disease and may be one step closer to producing patient-specific prevascularized tissues.

Financial & competing interests disclosure

The authors wish to disclose that RD Kamm has financial interests in AIM Biotech, a company that develops microfluidic systems similar to some of those described in this article. The authors wish to acknowledge the support from the NSF Science and Technology Center for Emergent Behaviors of Integrated Cellular Systems (CBET-0939511), the NIH (CA202177-01) and an NSERC post-doctoral fellowship to K Haase. The authors have no other relevant affiliations or financial involvement with any organization or entity with a financial interest in or financial conflict with the subject matter or materials discussed in the manuscript apart from those disclosed.

No writing assistance was utilized in the production of this manuscript.

References

Papers of special note have been highlighted as:
• of interest; •• of considerable interest

1 Novosel EC, Kleinhans C, Kluger PJ. Vascularization is the key challenge in tissue engineering. *Adv. Drug Del. Rev.* 63(4–5), 300–311 (2011).

2 Herbert SP, Stainier DYR. Molecular control of endothelial cell behaviour during blood vessel morphogenesis. *Nat. Rev. Mol. Cell Biol.* 12(9), 551–564 (2011).

3 Ferrara N, Gerber HP, Lecouter J. The biology of VEGF and its receptors. *Nat. Med.* 9(6), 669–676 (2003).

4 Carmeliet P, Jain RK. Angiogenesis in cancer and other diseases. *Nature* 407(6801), 249–257 (2000).

5 Tonini T, Rossi F, Claudio PP. Molecular basis of angiogenesis and cancer. *Oncogene* 22(42), 6549–6556 (2003).

6 Krock BL, Skuli N, Simon MC. Hypoxia-induced angiogenesis good and evil. *Genes Cancer* 2(12), 1117–1133 (2011).

7 Staton CA, Stribbling SM, Tazzyman S, Hughes R, Brown NJ, Lewis CE. Current methods for assaying angiogenesis *in vitro* and *in vivo*. *Int. J. Exp. Pathol.* 85(5), 233–248 (2004).

8 Nicosia RF, Ottinetti A. Growth of microvessels in serum-free matrix culture of rat aorta – a quantitative assay of angiogenesis *in vitro*. *Lab. Invest.* 63(1), 115–122 (1990).

9 Weinberg CB, Bell E. A blood-vessel model constructed from collagen and cultured vascular cells. *Science* 231(4736), 397–400 (1986).

10 Whitesides GM, Ostuni E, Takayama S, Jiang XY, Ingber DE. Soft lithography in biology and biochemistry. *Annu. Rev. Biomed. Eng.* 3, 335–373 (2001).

11 Chrobak KM, Potter DR, Tien J. Formation of perfused, functional microvascular tubes *in vitro*. *Microvasc. Res.* 71(3), 185–196 (2006).

12 Sadr N, Zhu MJ, Osaki T *et al.* SAM-based cell transfer to photopatterned hydrogels for microengineering vascular-like structures. *Biomaterials* 32(30), 7479–7490 (2011).

13 Yoshida H, Matsusaki M, Akashi M. Multilayered blood capillary analogs in biodegradable hydrogels for *in vitro* drug permeability assays. *Adv. Funct. Mater.* 23(14), 1736–1742 (2013).

14 Li X, Xu SL, He PN, Liu YX. *In vitro* recapitulation of functional microvessels for the study of endothelial shear response, nitric oxide and [Ca2+](i). *PLoS ONE* 10(5), e0126797 (2015).

15 Zheng Y, Chen JM, Craven M *et al. In vitro* microvessels for the study of angiogenesis and thrombosis. *Proc. Natl Acad. Sci. USA* 109(24), 9342–9347 (2012).

•• **A well-characterized example of endothelial cell (EC)-lined channels formed in an embedded collagen matrix, which allowed for the study of morphology, barrier function, interaction of EC and mural cells, flow and the antithrombotic response to whole blood.**

16 Heintz KA, Bregenzer ME, Mantle JL, Lee KH, West JL, Slater JH. Fabrication of 3D biomimetic microfluidic networks in hydrogels. *Adv. Healthc. Mater.* 30(10), 201600351 (2016).

17 Miller JS, Stevens KR, Yang MT *et al.* Rapid casting of patterned vascular networks for perfusable engineered three-dimensional tissues. *Nat. Mater.* 11(9), 768–774 (2012).

•• **Implemented a novel method to 3D print carbohydrate glass as a sacrificial template used to generate complex perfusable endothelial-lined microvessels.**

18 Zhang BY, Montgomery M, Chamberlain MD *et al.* Biodegradable scaffold with built-in vasculature for organ-on-a-chip engineering and direct surgical anastomosis. *Nat. Mater.* 15(6), 669–678 (2016).

•• **Developed an implantable AngioChip model using a degradable polymer that allows for angiogenic sprouting and anastomosis *in vivo*.**

19 Golden AP, Tien J. Fabrication of microfluidic hydrogels using molded gelatin as a sacrificial element. *Lab Chip* 7(6), 720–725 (2007).

20 Wang XY, Jin ZH, Gan BW, Lv SW, Xie M, Huang WH. Engineering interconnected 3D vascular networks

in hydrogels using molded sodium alginate lattice as the sacrificial templatet. *Lab Chip* 14(15), 2709–2716 (2014).

21 Tsang VL, Chen AA, Cho LM *et al.* Fabrication of 3D hepatic tissues by additive photopatterning of cellular hydrogels. *FASEB J.* 21(3), 790–801 (2007).

22 Brandenberg N, Lutolf MP. *In situ* patterning of microfluidic networks in 3D cell-laden hydrogels. *Adv. Mater.* 28(34), 7293–7547 (2016).

23 Huling J, Ko IK, Atala A, Yoo JJ. Fabrication of biomimetic vascular scaffolds for 3D tissue constructs using vascular corrosion casts. *Acta Biomater.* 32, 190–197 (2016).

24 El-Sherbiny IM, Yacoub MH. Hydrogel scaffolds for tissue engineering: progress and challenges. *Glob. Cardiol. Sci. Pract.* 2013(3), 316–342 (2013).

25 Folkman J. Tumor angiogenesis - possible control point in tumor-growth. *Ann. Intern. Med.* 82(1), 96–100 (1975).

26 Folkman J. Tumor angiogenesis factor. *Cancer Res.* 34(8), 2109–2113 (1974).

27 Ribatti D. Judah Folkman, a pioneer in the study of angiogenesis. *Angiogenesis* 11(1), 3–10 (2008).

28 Song JW, Munn LL. Fluid forces control endothelial sprouting. *Proc. Natl Acad. Sci. USA* 108(37), 15342–15347 (2011).

29 Farahat WA, Wood LB, Zervantonakis IK *et al.* Ensemble analysis of angiogenic growth in three-dimensional microfluidic cell cultures. *PLoS ONE* 7(5), e37333 (2012).

30 Nguyen DH, Stapleton SC, Yang MT *et al.* Biomimetic model to reconstitute angiogenic sprouting morphogenesis *in vitro*. *Proc. Natl Acad. Sci. USA* 110(17), 6712–6717 (2013).

31 Vickerman V, Kamm RD. Mechanism of a flow-gated angiogenesis switch: early signaling events at cell–matrix and cell–cell junctions. *Integr. Biol.* 4(8), 863–874 (2012).

32 Nehls V, Drenckhahn D. A microcarrier-based cocultivation system for the investigation of factors and cells involved in angiogenesis in 3-dimensional fibrin matrices *in-vitro*. *Histochem. Cell Biol.* 104(6), 459–466 (1995).

33 Nakatsu MN, Sainson RCA, Aoto JN *et al.* Angiogenic sprouting and capillary lumen formation modeled by human umbilical vein endothelial cells (HUVEC) in fibrin gels: the role of fibroblasts and Angiopoietin-1. *Microvasc. Res.* 66(2), 102–112 (2003).

34 Newman AC, Nakatsu MN, Chou W, Gershon PD, Hughes CCW. The requirement for fibroblasts in angiogenesis: fibroblast-derived matrix proteins are essential for endothelial cell lumen formation. *Mol. Biol. Cell.* 22(20), 3791–3800 (2011).

35 Mcdonald JC, Duffy DC, Anderson JR *et al.* Fabrication of microfluidic systems in poly(dimethylsiloxane). *Electrophoresis* 21(1), 27–40 (2000).

36 Yeon JH, Ryu HR, Chung M, Hu QP, Jeon NL. *In vitro* formation and characterization of a perfusable three-dimensional tubular capillary network in microfluidic devices. *Lab Chip* 12(16), 2815–2822 (2012).

37 Vickerman V, Blundo J, Chung S, Kamm R. Design, fabrication and implementation of a novel multi-parameter control microfluidic platform for three-dimensional cell culture and real-time imaging. *Lab Chip* 8(9), 1468–1477 (2008).

38 Dai BL, Zhang YM, Zhan YZ, Zhang DD, Wang N, He LC. A novel tissue model for angiogenesis: evaluation of inhibitors or promoters in tissue level. *Sci. Rep.* 4, 3693 (2014).

39 Jeon JS, Bersini S, Whisler JA *et al.* Generation of 3D functional microvascular networks with human mesenchymal stem cells in microfluidic systems. *Integr. Biol.* 6(5), 555–563 (2014).

40 Hsu YH, Moya ML, Hughes CCW, George SC, Lee AP. A microfluidic platform for generating large-scale nearly identical human microphysiological vascularized tissue arrays. *Lab Chip* 13(15), 2990–2998 (2013).

41 Chung S, Sudo R, Mack PJ, Wan CR, Vickerman V, Kamm RD. Cell migration into scaffolds under co-culture conditions in a microfluidic platform. *Lab Chip* 9(2), 269–275 (2009).

42 Du Y, Herath SCB, Wang QG, Wang DA, Asada HH, Chen PCY. Three-dimensional characterization of mechanical interactions between endothelial cells and extracellular matrix during angiogenic sprouting. *Sci. Rep.* 6, 21362 (2016).

43 Shamloo A, Ma N, Poo MM, Sohn LL, Heilshorn SC. Endothelial cell polarization and chemotaxis in a microfluidic device. *Lab Chip* 8(8), 1292–1299 (2008).

44 Lim SH, Kim C, Aref AR, Kamm RD, Raghunath M. Complementary effects of ciclopirox olamine, a prolyl hydroxylase inhibitor and sphingosine 1-phosphate on fibroblasts and endothelial cells in driving capillary sprouting. *Integr. Biol.* 5(12), 1474–1484 (2013).

45 Herland A, Van Der Meer AD, Fitzgerald EA, Park TE, Sleeboom JJF, Ingber DE. Distinct contributions of astrocytes and pericytes to neuroinflammation identified in a 3D human blood-brain barrier on a chip. *PLoS ONE* 11(3), e0150360 (2016).

46 Bischel LL, Young EWK, Mader BR, Beebe DJ. Tubeless microfluidic angiogenesis assay with three-dimensional endothelial-lined microvessels. *Biomaterials* 34(5), 1471–1477 (2013).

47 Belair DG, Whisler JA, Valdez J *et al.* Human vascular tissue models formed from human induced pluripotent stem cell derived endothelial cells. *Stem Cell Rev. Rep.* 11(3), 511–525 (2015).

• **Demonstrated the use of induced pluripotent stem cell-ECs as a potential cell source for generating perfusable *in vitro* microvascular networks.**

48 Whisler JA, Chen MB, Kamm RD. Control of perfusable microvascular network morphology using a multiculture microfluidic system. *Tissue Eng. Part C Methods* 20(7), 543–552 (2014).

•• **Uses a microfluidic gel-channel model of vasculogenesis to characterize network growth and long-term stability, which is shown to depend crucially on mural cells.**

49 Kim S, Lee H, Chung M, Jeon NL. Engineering of functional, perfusable 3D microvascular networks on a chip. *Lab Chip* 13(8), 1489–1500 (2013).

•• **Perfusable networks generated using a parallel gel-channel model are shown to respond to shear flow by cytoskeletal reorganization and nitrous oxide synthesis.**

50 Moya ML, Hsu YH, Lee AP, Hughes CCW, George SC. *In vitro* perfused human capillary networks. *Tissue Eng. Part C Methods* 19(9), 730–737 (2013).

• **Produces arrays of mechanically similar vascularized and perfusable networks, with the ability to control pressure gradients and flow during 2–3 week culture periods.**

51 Chen MB, Whisler JA, Jeon JS, Kamm RD. Mechanisms of tumor cell extravasation in an *in vitro* microvascular network platform. *Integr. Biol.* 5(10), 1262–1271 (2013).

•• **Employs an *in vitro* gel-channel microfluidic microvascular model to examine extravasation of cancer cells.**

52 Wang XL, Phan DTT, Sobrino A, George SC, Hughes CCW, Lee AP. Engineering anastomosis between living capillary networks and endothelial cell-lined microfluidic channels. *Lab Chip* 16(2), 282–290 (2016).

53 Rosenfeld D, Landau S, Shandalov Y *et al.* Morphogenesis of 3D vascular networks is regulated by tensile forces. *Proc. Natl Acad. Sci. USA* 113(12), 3215–3220 (2016).

54 Zhou XP, He PN. Endothelial [Ca2+](i) and caveolin-1 antagonistically regulate eNOS activity and microvessel permeability in rat venules. *Cardiovasc. Res.* 87(2), 340–347 (2010).

55 Radu M, Chernoff J. An *in vivo* assay to test blood vessel permeability. *J. Vis. Exp.* (73), e50062 (2013).

56 Huxley VH, Curry FE, Adamson RH. Quantitative fluorescence microscopy on single capillaries – alpha-lactalbumin transport. *Am. J. Physiol.* 252(1), H188–H197 (1987).

57 Tarbell JM. Shear stress and the endothelial transport barrier. *Cardiovasc. Res.* 87(2), 320–330 (2010).

58 Curry FRE, Adamson RH. Vascular permeability modulation at the cell, microvessel, or whole organ level: towards closing gaps in our knowledge. *Cardiovasc. Res.* 87(2), 218–229 (2010).

59 Morgan JP, Delnero PF, Zheng Y *et al.* Formation of microvascular networks *in vitro*. *Nat. Protoc.* 8(9), 1820–1836 (2013).

60 Price GM, Chrobak KM, Tien J. Effect of cyclic AMP on barrier function of human lymphatic microvascular tubes. *Microvasc. Res.* 76(1), 46–51 (2008).

61 Choi NW, Cabodi M, Held B, Gleghorn JP, Bonassar LJ, Stroock AD. Microfluidic scaffolds for tissue engineering. *Nat. Mater.* 6(11), 908–915 (2007).

62 Wu NZ, Klitzman B, Rosner G, Needham D, Dewhirst MW. Measurement of material extravasation in microvascular networks using fluorescence video-microscopy. *Microvasc. Res.* 46(2), 231–253 (1993).

63 Gerlowski LE, Jain RK. Microvascular permeability of normal and neoplastic tissues. *Microvasc. Res.* 31(3), 288–305 (1986).

64 Yuan W, Lv YG, Zeng M, Fu BM. Non-invasive measurement of solute permeability in cerebral microvessels of the rat. *Microvasc. Res.* 77(2), 166–173 (2009).

65 Price GM, Wong KHK, Truslow JG, Leung AD, Acharya C, Tien J. Effect of mechanical factors on the function of engineered human blood microvessels in microfluidic collagen gels. *Biomaterials* 31(24), 6182–6189 (2010).

66 Lai VK, Lake SP, Frey CR, Tranquillo RT, Barocas VH. Mechanical behavior of collagen-fibrin co-gels reflects transition from series to parallel interactions with increasing collagen content. *J. Biomech. Eng.* 134(1), 011004 (2012).

67 Munster S, Jawerth LM, Leslie BA, Weitz JI, Fabry B, Weitz DA. Strain history dependence of the nonlinear stress response of fibrin and collagen networks. *Proc. Natl Acad. Sci. USA* 110(30), 12197–12202 (2013).

68 Kannan RY, Salacinski HJ, Sales K, Butler P, Seifalian AM. The roles of tissue engineering and vascularisation in the development of micro-vascular networks: a review. *Biomaterials* 26(14), 1857–1875 (2005).

69 Dai XZ, Cai SX, Ye QF *et al.* A novel *in vitro* angiogenesis model based on a microfluidic device. *Chin. Sci. Bull.* 56(31), 3301–3309 (2011).

70 Yamashita J, Itoh H, Hirashima M *et al.* Flk1-positive cells derived from embryonic stem cells serve as vascular progenitors. *Nature* 408(6808), 92–96 (2000).

71 Orekhov AN, Bobryshev YV, Chistiakov DA. The complexity of cell composition of the intima of large arteries: focus on pericyte-like cells. *Cardiovasc. Res.* 103(4), 438–451 (2014).

72 Sekine H, Shimizu T, Sakaguchi K *et al. In vitro* fabrication of functional three-dimensional tissues with perfusable blood vessels. *Nat. Commun.* 4, 1399 (2013).

73 Mishra A, O'farrell FM, Reynell C, Hamilton NB, Hall CN, Attwell D. Imaging pericytes and capillary diameter in brain slices and isolated retinae. *Nat. Protoc.* 9(2), 323–336 (2014).

74 Levenberg S, Rouwkema J, Macdonald M *et al.* Engineering vascularized skeletal muscle tissue. *Nat. Biotechnol.* 23(7), 879–884 (2005).

75 Szymanski MP, Metaxa E, Meng H, Kolega J. Endothelial cell layer subjected to impinging flow mimicking the apex of an arterial bifurcation. *Ann. Biomed. Eng.* 36(10), 1681–1689 (2008).

76 Dobrin PB. Mechanical-properties of arteries. *Physiol. Rev.* 58(2), 397–460 (1978).

77 Kovacs G, Berghold A, Scheidl S, Olschewski H. Pulmonary arterial pressure during rest and exercise in healthy subjects: a systematic review. *Eur. Respir. J.* 34(4), 888–894 (2009).

78 Barrett HE, Cunnane EM, Kavanagh EG, Walsh MT. Towards the characterisation of carotid artery plaque: linking mechanical properties to biological content. *Ir. J. Med. Sci.* 185, S85–S85 (2016).

79 Learoyd BM, Taylor MG. Alterations with age in the viscoelastic properties of human arterial walls. *Circ. Res.* 18(3), 278–292 (1966).

80 Lawrence AR, Gooch KJ. Transmural pressure and axial loading interactively regulate arterial remodeling *ex vivo*. *Am. J. Physiol. Heart Circ. Physiol.* 297(1), H475–H484 (2009).

81 Tzima E, Irani-Tehrani M, Kiosses WB *et al.* A mechanosensory complex that mediates the endothelial cell response to fluid shear stress. *Nature* 437(7057), 426–431 (2005).

82 Shay-Salit A, Shushy M, Wolfovitz E *et al.* VEGF receptor 2 and the adherens junction as a mechanical transducer in vascular endothelial cells. *Proc. Natl Acad. Sci. USA* 99(14), 9462–9467 (2002).

83 Ostrowski MA, Huang NF, Walker TW *et al.* Microvascular endothelial cells migrate upstream and align against the shear stress field created by impinging flow. *Biophys. J.* 106(2), 366–374 (2014).

84 Sato M, Saito N, Sakamoto N, Ohashi T. High wall shear stress gradient suppress morphological responses of endothelial cells to fluid flow. *Ifmbe Proc.* 25, 312–313 (2010).

85 Kim S, Chung M, Jeon NL. Three-dimensional biomimetic model to reconstitute sprouting lymphangiogenesis *in vitro*. *Biomaterials* 78, 115–128 (2016).

86 Xiong Y, Hu ZQ, Han XF *et al.* Hypertensive stretch regulates endothelial exocytosis of Weibel-Palade bodies through VEGF receptor 2 signaling pathways. *Cell Res.* 23(6), 820–834 (2013).

87 Jufri NF, Mohamedali A, Avolio A, Baker MS. Mechanical stretch: physiological and pathological implications for human vascular endothelial cells. *Vasc. Cell* 7, 8 (2015).

88 Huang R, Zheng WF, Liu WW, Zhang W, Long YZ, Jiang XY. Investigation of tumor cell behaviors on a vascular microenvironment-mimicking microfluidic chip. *Sci. Rep.* 5, 17768 (2015).

89 Huh D, Matthews BD, Mammoto A, Montoya-Zavala M, Hsin HY, Ingber DE. Reconstituting organ-level lung functions on a chip. *Science* 328(5986), 1662–1668 (2010).

90 Booth R, Kim H. Characterization of a microfluidic *in vitro* model of the blood-brain barrier (muBBB). *Lab Chip* 12(10), 1784–1792 (2012).

91 Sobrino A, Phan DTT, Datta R *et al.* 3D microtumors *in vitro* supported by perfused vascular networks. *Sci. Rep.* 6, 31589 (2016).

92 Bhatia SN, Ingber DE. Microfluidic organs-on-chips. *Nat. Biotechnol.* 32(8), 760–772 (2014).

93 Wagner I, Materne EM, Brincker S *et al.* A dynamic multi-organ-chip for long-term cultivation and substance testing proven by 3D human liver and skin tissue co-culture. *Lab Chip* 13(18), 3538–3547 (2013).

94 Halldorsson S, Lucumi E, Gomez-Sjoberg R, Fleming RMT. Advantages and challenges of microfluidic cell culture in polydimethylsiloxane devices. *Biosens. Bioelectron.* 63, 218–231 (2015).

95 Rai R, Tallawi M, Grigore A, Boccaccini AR. Synthesis, properties and biomedical applications of poly(glycerol sebacate) (PGS): a review. *Prog. Polym. Sci.* 37(8), 1051–1078 (2012).

96 Hoffman AS. Hydrogels for biomedical applications. *Adv. Drug Del. Rev.* 64, 18–23 (2012).

97 Cao YL, Vacanti JP, Paige KT, Upton J, Vacanti CA. Transplantation of chondrocytes utilizing a polymer-cell construct to produce tissue-engineered cartilage in the shape of a human ear. *Plast. Reconstr. Surg.* 100(2), 297–302 (1997).

98 Bertassoni LE, Cecconi M, Manoharan V *et al.* Hydrogel bioprinted microchannel networks for vascularization of tissue engineering constructs. *Lab Chip* 14(13), 2202–2211 (2014).

99 Kolesky DB, Truby RL, Gladman AS, Busbee TA, Homan KA, Lewis JA. 3D bioprinting of vascularized, heterogeneous cell-laden tissue constructs. *Adv. Mater.* 26(19), 3124–3130 (2014).

100 Kinstlinger IS, Miller JS. 3D-printed fluidic networks as vasculature for engineered tissue. *Lab Chip* 16(11), 2025–2043 (2016).